MRI of the Wrist

Donald von Borstel, D.O.,[1] Saya Horiuchi, M.D.,[2] Nicholas Strle, D.O.,[1] Hiroshi Yoshioka, M.D., Ph.D.[2]

[1]Department of Radiology, Oklahoma State University Medical Center, Tulsa, OK
[2]Department of Radiological Sciences, University of California, Irvine, Orange, CA

Wrist pain is a common clinical presentation and the specific diagnosis is often challenging to obtain with clinical evaluation and radiography alone. If the patient's initial radiographs are noncontributory to the diagnosis, further imaging is often necessary. MRI utilization has progressively increased due to a variety of factors, including more athletic pursuits in children that may cause wrist injury, widespread availability of MRI, and improved diagnostic capabilities of wrist MRI. Therefore, MRI is a key diagnostic modality that can heavily influence treatment decisions, making it essential that radiologists effectively diagnose common wrist disorders. This review article focuses on MRI assessment of the wrist, including ligamentous injuries, carpal fractures, and various tendon pathologies, as well as patterns of advanced collapse and avascular necrosis affecting the wrist.

Ligamentous Injury

Imaging wrist ligaments is often challenging because they are thin and have an oblique course. The wrist ligaments are commonly divided into intrinsic and extrinsic ligaments. The intrinsic ligaments attach solely to the carpal bones, whereas the extrinsic ligaments connect the ulna, radius, or metacarpals to the carpal bones.[1] They are both important for maintaining carpal stability, with intrinsic ligaments being the primary stabilizers.[2]

Intrinsic Ligaments

The scapholunate ligament (SLL) and lunotriquetral ligament (LTL) are essential for stability of the proximal carpal row.[3] For accurate injury assessment, one must be familiar with their normal variation in morphology and signal intensity.[1]

Scapholunate Ligament Injury— The SLL is horseshoe shaped with 3 components: the volar, dorsal and proximal zones. The dorsal component is approximately 3 mm thick and is associated with the joint capsule. The dorsal component is the most critical in preserving the relationship between the proximal poles of the scaphoid and the lunate.[4] The volar component is ligamentous and thinner than the dorsal component. The proximal component is the weakest and most susceptible to degenerative perforation.

MRI or MR arthrography (MRA) is of great importance in assessing the SLL. On axial images, the dorsal component is a thick, band-like structure with low signal intensity, whereas the volar component is heterogeneous (**Figure 1**). The proximal zone is best seen on coronal images. Although the proximal component of the SLL has a relatively similar triangular shape, it has a wide variety in shape (**Figure 2**). Isolated asymptomatic proximal defects are common in adults.[2] Tears of the SLL are diagnosed on MRI with findings of irregular morphology, abnormal signal intensity, and fluid transecting the ligaments.[1] A meta-analysis of the major diagnostic accuracy studies reported that the overall sensitivity and specificity of 3T-MRI for SLL tears were 75.5% and 97.1%, respectively. The sensitivity and specificity of MRA were reported as 82.1% and 92.8%, respectively.[5]

Scapholunate dissociation does not occur with disruption of the dorsal component of the SLL alone. Rather, the SLL injury in combination with injury to portions of the dorsal and volar extrinsic ligaments results in the dorsiflexed intercalated segment instability (DISI) deformity with flexion of the scaphoid and extension of the lunate and triquetrum.[6]

Lunotriquetral Ligament Injury— The LTL appears V-shaped and like the SLL, consists of the volar, dorsal and proximal zones. The dorsal component is the most important in carpal stability and resistance to rotation.[4]

The volar and dorsal zones appear band-like on axial images traversing

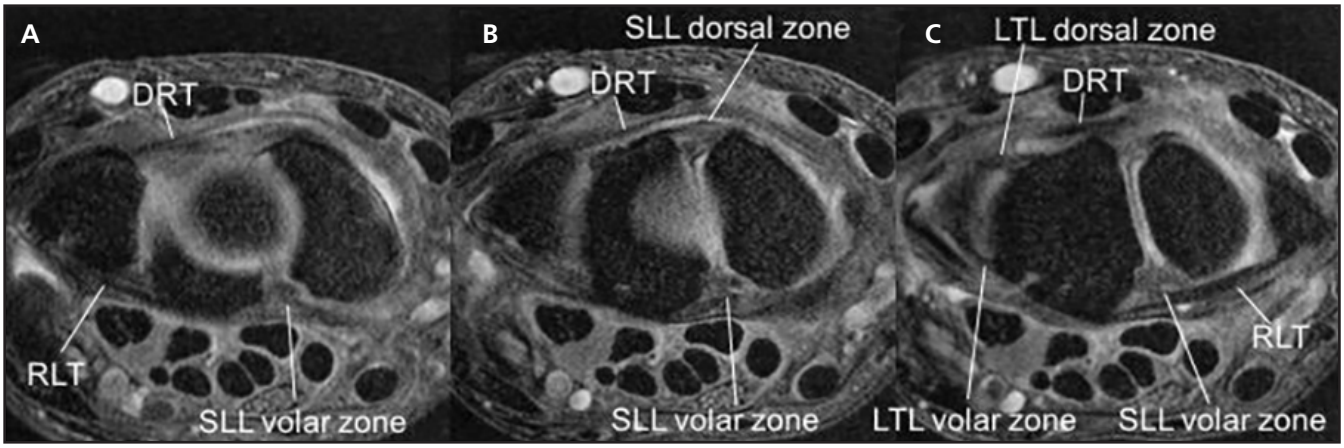

FIGURE 1. *The intrinsic and extrinsic ligaments on axial fat-suppressed (FS) proton density-weighted images (PDWI). The volar zone of the SLL shows inhomogeneous striate structure (A-C), whereas the dorsal zone of the SLL appears as a thick and band-like structure (B). The volar and dorsal zones of the LTL appear band-like and have linear shapes running in the interspace between the lunate and triquetrum (C). The RLT and DRT are hypointense band-like structures (A-C).*

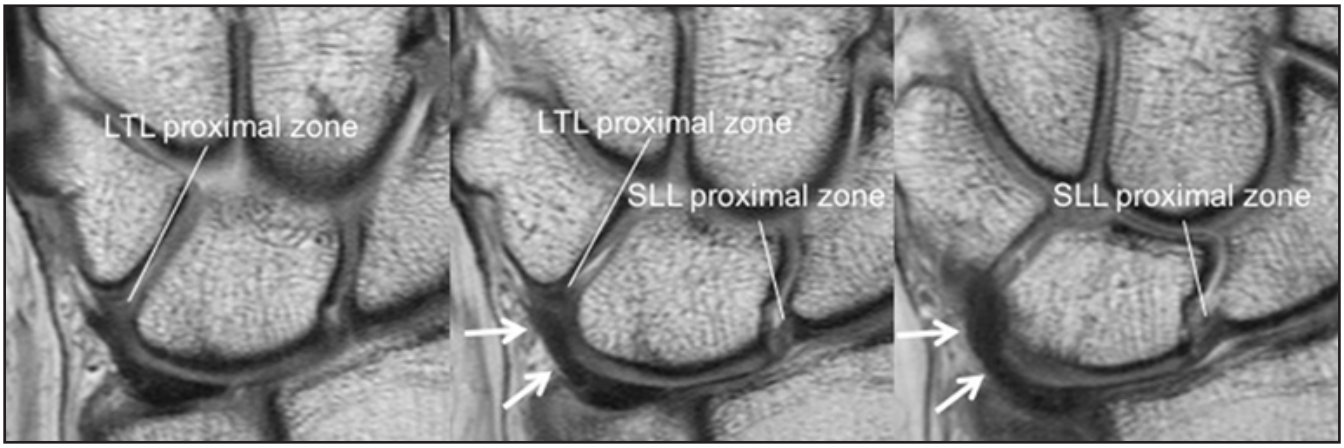

FIGURE 2. *The intrinsic ligaments on coronal PDWI. The proximal zones of the SLL and LTL show triangular shapes. Arrows show the ulnotriquetral ligament.*

between the lunate and triquetrum **(Figure 1)**. The proximal zone is best seen on coronal images with a triangular appearance **(Figure 2)**. Half of adults older than age 50 have communicating defects in the proximal zone of the LTL.[2] A few recent studies with small numbers of patients have compared the accuracy of MRI/MRA with arthroscopy. Sensitivity and specificity of MRI in detecting a complete LTL tear were 0% to 82% and 93% to 100%,[7] respectively; whereas sensitivity and specificity of MRA were 100% and 94% to 100%, respectively.[8]

LTL injuries are a common cause of ulnar-sided wrist pain and occur with a fall onto an extended, pronated, and radial deviated hand.[9] Degenerative LTL tears will result from chronic ulnar impaction syndrome.[10] Ulnar impaction syndrome is a progressive degenerative wrist condition that occurs secondary to excessive load across the ulnocarpal joint, resulting in a degenerative triangular fibrocartilage complex (TFCC) tear, disruption of the LTL, and chondromalacia of the ulna, lunate and triquetrum. Therefore, in the setting of degenerative TFCC tears, LTL lesions require careful assessment.[9]

Extrinsic Ligaments

Extrinsic ligament injuries can cause carpal instability and chronic wrist pain, especially when combined with intrinsic ligament injuries. An MR study of wrist trauma showed that 75% of patients had extrinsic ligament injuries, 60% had intrinsic ligament injuries, and almost half had combined ligamentous injuries.[11] Early ligament studies focused on only volar extrinsic ligaments; however, there is mounting evidence that both volar and dorsal capsular ligaments contribute to carpal function and alignment.[2]

Volar Extrinsic Ligaments— There are 3 major volar extrinsic ligaments: the radioscaphocapitate (RSC), radiolunotriquetral (RLT), and short radiolunate (SRL) ligaments (**Figure 3**). The RSC arises from the radial styloid process volar surface, supports the scaphoid waist, and inserts to the capitate. The RSC supports scaphoid stability acting as a "seat belt" at the scaphoid waist.[2] The RLT arises from the radial styloid process volar rim, passes volar to the proximal scaphoid pole, attaches to the volar surface of the lunate, and inserts onto the triquetrum.[2]

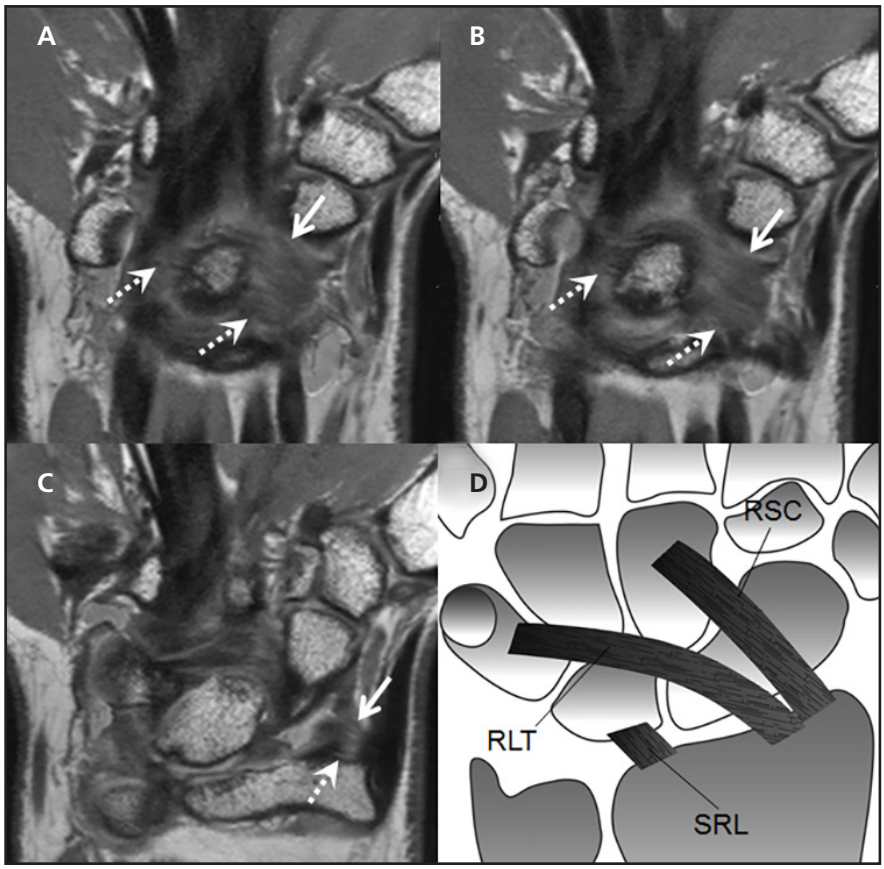

FIGURE 3. *The volar extrinsic ligaments on coronal isotropic 3D PDWI (A, B, C) and a diagram of the volar extrinsic ligaments (D): RSC (solid arrows), RLT (dashed arrows), and SRL ligaments. Both RSC and RLT show a striated appearance (A-C).*

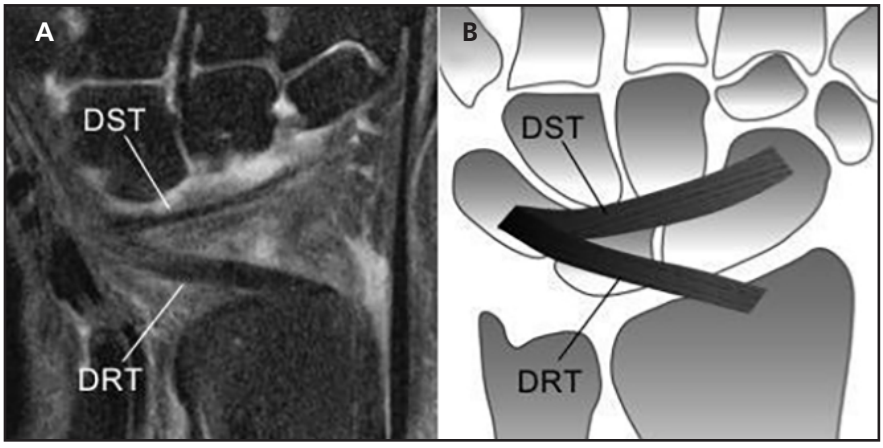

FIGURE 4. *The dorsal carpal ligaments on a coronal FS PDWI (A) and a diagram of the dorsal ligaments (B): the DRT and DST ligaments form a V-shape with the apex pointed toward the triquetrum.*

The RLT is clinically important for load transference and preventing ulnar translation of the carpus.[2] The SRL arises from the volar-ulnar aspect of the radius and attaches to the volar aspect of the lunate. Therefore, both RLT and SRL strongly anchor the lunate to the radius.

The normal RSC and RLT can be identified as linear hypointense structures with striated bands of intermediate signal intensity (**Figure 3**), whereas the SRL appears as a homogeneously hypointense focal thickening of the volar joint capsule. In the setting of trauma, the most frequently injured extrinsic ligaments were the RLT and RSC, almost half of which were associated with scaphoid injury.[11]

Dorsal Extrinsic Ligaments— Two major dorsal ligaments provide radioscaphoid stability—the dorsal radiotriquetral (DRT) and dorsal scaphotriquetral (DST) ligaments (**Figure 4**). These ligaments form a V-shape with the apex to the triquetrum, and can be identified as linear hypointense structures, often with striated bands of intermediate signal intensity (**Figure 4**).[2] The DRT was shown to be the third most frequently injured extrinsic ligament, and is commonly involved in triquetrum avulsions.[11]

Triangular Fibrocartilage Complex (TFCC)

The TFCC is a fibrocartilage-ligament complex providing stability to the distal radioulnar joint and helps transmit axial load from the carpus to the ulna. The TFCC is an essential pivot point for forearm rotation and is highly prone to injuries.[12] The TFCC is comprised of an articular disc (TFC disc proper) and surrounding fibrous structures—the triangular ligament, the volar and dorsal radioulnar ligaments, the ulnolunate ligament, the ulnotriquetral ligament, the ulnar collateral ligament, and the meniscus homologue (**Figure 5**).[13] The triangular ligament has V-shaped collagen fiber bundles, which anchor the fibrocartilaginous disc proper to the tip and fovea/base of the ulnar styloid process. The volar and dorsal radioulnar ligaments form the volar and dorsal margins of the TFCC. The volar radioulnar ligament is reinforced by ulnolunate and ulnotriquetral ligaments inserting to the volar lunate and triquetrum, respectively. Although the structural terminology is still controversial, the extensor carpi ulnaris (ECU) tendon subsheath can be included as a stabilizer of the ulnar side of the TFCC. The ECU tendon changes in position between supination and pronation.[14]

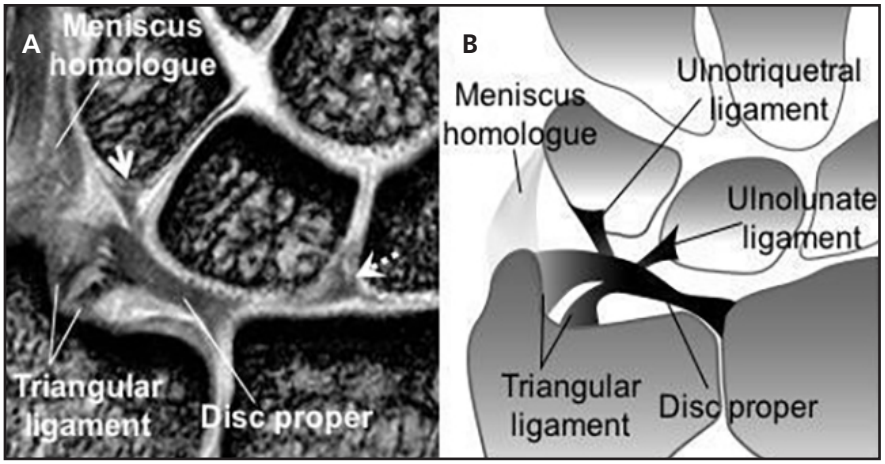

FIGURE 5. *TFCC on a coronal gradient echo T2-weighted image (A) and a diagram of the TFCC (B). The image was obtained using a 47-mm microscopy coil. The normal disc proper shows asymmetric bowtie-like low signal intensity, whereas the triangular ligament shows a striated pattern of increased internal signal. The meniscus homologue arises from the tip of the ulnar styloid process, and attaches to the ulnar side of the triquetrum and lunate. Dotted arrow shows the proximal zone of the SLL. Solid arrow shows the LTL.*

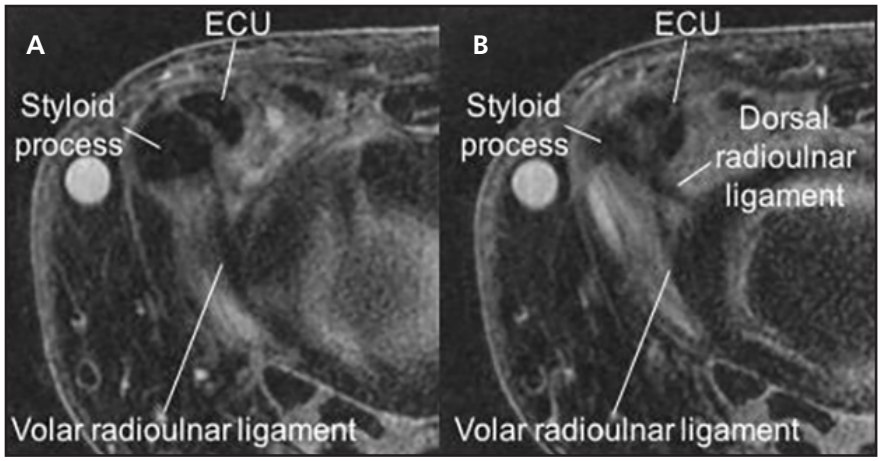

FIGURE 6*. The TFCC in neutral position on axial FS PDWI (A and B). The volar and dorsal radioulnar ligaments show hypointense band-like structures. In neutral position, the ECU tendon travels dorsally and medially to the ulnar styloid process.*

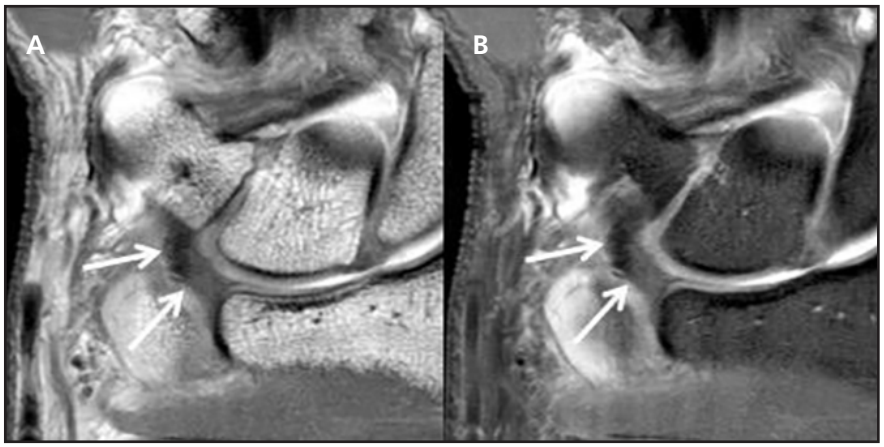

FIGURE 7. *The ulnotriquetral ligament on a coronal PDWI (A) and a coronal FS PDWI (B). The ulnotriquetral ligament arises from the disc proper and inserts to the volar surface of the triquetrum (arrows).*

On coronal images, the normal disc proper shows asymmetric bowtie-like low signal intensity, whereas the triangular ligament shows a striated pattern of increased internal signal (**Figure 5**).[15] On axial images, the volar and dorsal radioulnar ligaments are well recognized as hypointense band-like structures (**Figure 6**). The ulnolunate and ulnotriquetral ligaments show homogeneous low-signal intensity (**Figure 7**).

Noncontrast MRI studies have shown that the overall sensitivity and specificity for TFCC injuries were 83% and 82%, respectively.[16] MRA was superior to noncontrast MRI in an investigation of TFCC injuries, with an overall sensitivity of 84% and specificity of 95%.[17]

MR Technique for Evaluation of the TFCC

Appropriate MRI techniques should be applied for visualization of precise TFCC anatomy. **Table 1** shows a detailed overview of the typical routine sequence protocols for 3T-imaging of the wrist.[14] Images have commonly been acquired with conventional 2-dimensional (2D) techniques; however, 3D-imaging techniques reduce partial volume artifact and can be reformatted into any cross-sectional plane from a single acquisition. Although the isotropic 3D fast spin echo (FSE) sequences suffer from relatively long acquisition time and image blurring, several advanced techniques—such as parallel imaging, short TR sequences combined with driven equilibrium, and compressed sensing—have shortened overall scan time.[18]

Traumatic TFCC Tears

The Palmer classification divides TFCC tears into traumatic and degenerative lesions (**Table 2**).[19] This classification system is frequently used by hand surgeons to guide management.[13]

Traumatic tears occur far less frequently than degenerative tears. The most common mechanism of traumatic TFCC injury is a fall on an outstretched

Table 1. Routine MR Parameters for 3T Imaging of the Wrist[14]

Sequence	Cor 3D PD FS	Cor PD	Cor PD FS	Ax PD	Ax PDFS/ Ax T_2FS	Sag PD	Sag PD FS
Pixel size (mm × mm)	0.35 × 0.35	0.27 × 0.35	0.30 × 0.32	0.4 × 0.4	0.32 × 0.44	0.40 × 0.51	0.23 × 0.32
Slice thickness (mm)	0.35	2	2	2	2	3	3
Slice gap (mm)	0	0.2	0.2	0.2	0.2	0.3	0.3
Number of slices	151	22	22	30	30	22	20-30
FOV (mm)	70	90	90	80	80	70-80	70-80
TE (ms)	29-37	30	27	30	30/70	30	27
TR (ms)	1250-1400	3500	2500-3500	2500	3000/3200	3000	2500-3500
BW (Hz/pixel)	362	194	222	250	153/218	354	175
Echo train length	70-88	13	13	9	11	12	13
NEX	2	1	3	2	2	1	1
Acquisition time (min)	~5	~2.5	~4	~3	~2.5/3	~2.8	~3.5

Key: Ax = axial; Cor = coronal; Sag = sagittal; 3D = 3-dimensional; PD = proton-density; FS = fat-suppression; FOV = field-of-view; TE = echo time; TR = repetition time; BW = bandwidth; NEX = number of excitations
Table 1 from reference 14, reproduced with permission.

Table 2. Palmer Injury Classification for the TFCC

Class I (Traumatic)
- A. Central perforation
- B. Ulnar avulsion
- C. Distal avulsion
- D. Radial avulsion

Class II (Degenerative)
- A. TFCC wear
- B. TFCC wear with lunate and/or ulnar chondromalacia
- C. TFCC perforation with lunate and/or ulnar chondromalacia
- D. C and LTL perforation
- E. D and ulnocarpal arthritis

hand. TFCC tears usually present clinically as ulnar-sided wrist pain and/or distal radioulnar joint instability.

Class I/traumatic TFCC tears are subclassified according to injury location. Conservative treatments are generally recommended; when conservative management is unsuccessful, several surgical options can be considered. The surgical treatments can be based on the TFCC lesion location. Class IA tear is at the central/paracentral region of the disc proper, which is the most common traumatic subtype of TFCC tears (**Figure 8**). Since the avascular central articular disc has limited healing capacity, debridement is usually performed for pain relief.[20] Class 1B tear is the avulsion of the triangular ligament with or without an ulnar styloid fracture (**Figure 9**). The instability of the distal radioulnar joint is most remarkable in Class IB injuries. Class IC tear is avulsion of the ulnolunate or ulnotriquetral ligaments, which can result in ulnocarpal instability. For Class IB and IC injuries, surgical repair may be indicated.[20] A Class ID tear involves either an avulsion tear of the

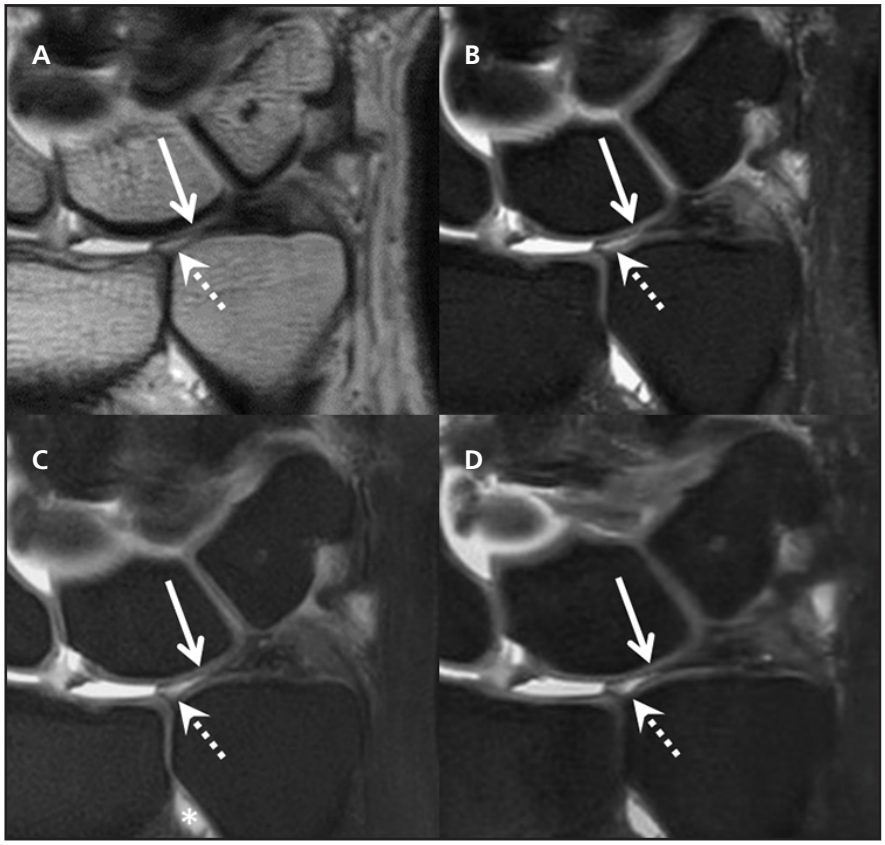

FIGURE 8. *Class IA and ID traumatic lesions of the TFCC on MR arthrogram with axial PDWI (A), FS PDWI (B), FS T1-weighted image (T1WI) (C), and isotropic 3D FS PDWI (D). There is an extensive tear of the central disc proper (solid arrow) and avulsion of the radial attachment (dashed arrows). Contrast is seen leaking through the distal radioulnar joint (asterisk image C). Class IA is the most common subtype of TFCC traumatic tears.*

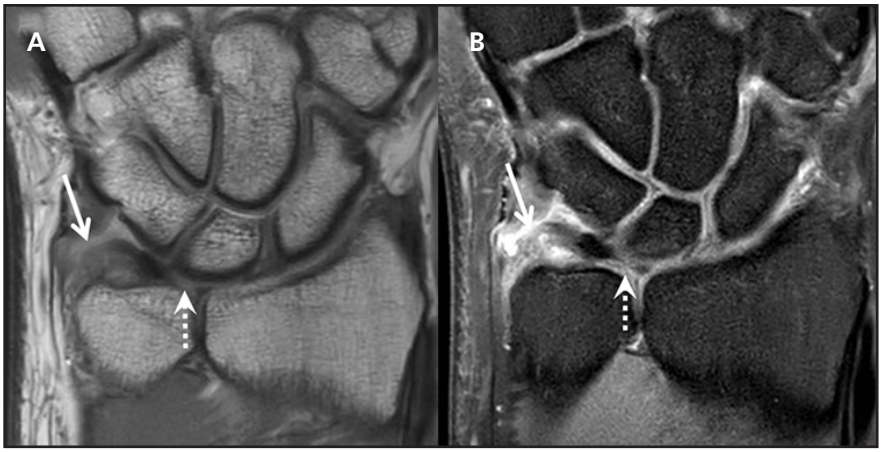

FIGURE 9. *Class IB traumatic lesion of the TFCC. PDWI (A) shows an ulnar styloid triangular ligament tear (solid arrow). FS PDWI (B) shows the hyperintense signal of the triangular ligament tear (arrow). Class IB tears involve avulsion of the triangular ligament and can occur with or without a styloid process fracture. An incidental perforation of the central disc is consistent with a concomitant Class IA lesion (dashed arrow in A and B).*

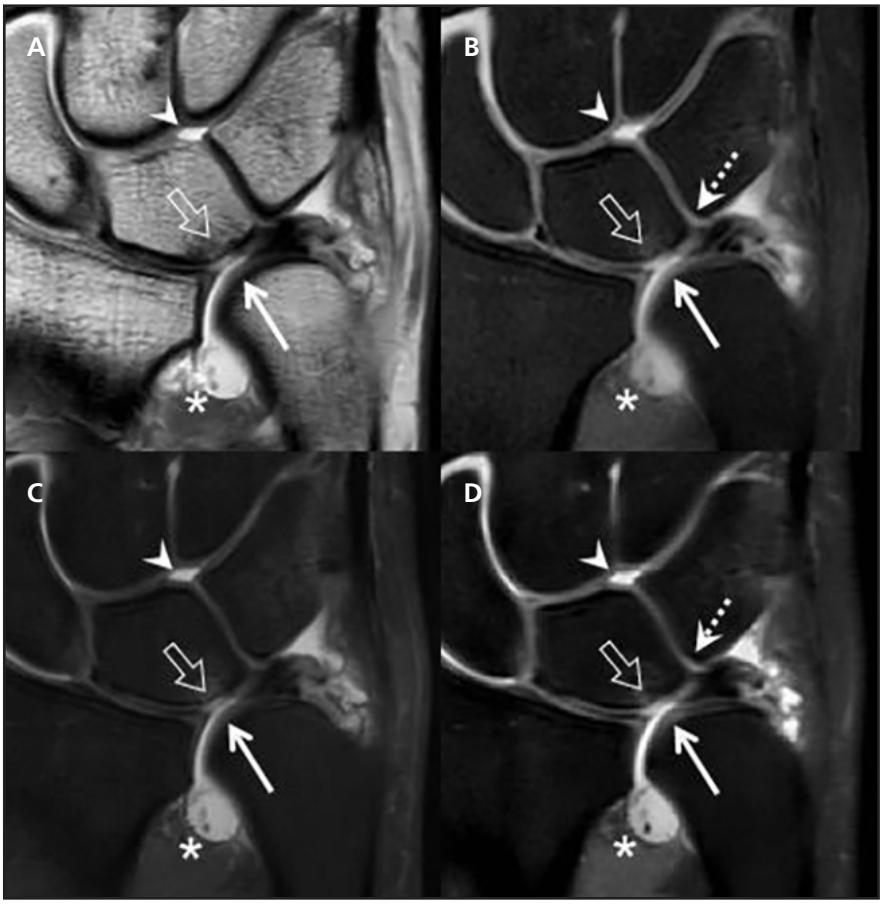

FIGURE 10. *Degeneration with perforation of the central disc of the TFCC, chondromalacia of the lunate, and LTL perforation (Palmer Class IID). MRA coronal PDWI (A), coronal FS T1WI (B), coronal FS PDWI (C), and isotropic 3D coronal FS PDWI (D) show perforation of the central disc (solid arrows) and a full thickness cartilage defect and subchondral bone marrow edema of the lunate (open arrows). A small and irregularly shaped LTL with oblique linear high-signal (contrast) through its proximal portion (dotted arrows) is visualized in (B) and (D), and intra-articular contrast extends into the midcarpal joint (arrowheads), suggesting the LTL perforation. The contrast material also extends into the distal radioulnar joint, suggesting the disc injury (asterisk).*

TFCC (**Figure 8**) or an avulsion fracture at the sigmoid notch of the radius. When the avulsion fracture exists, a direct repair leads to better outcomes.[20] For a Class ID tear without avulsion fracture, various surgical repairs have been reported and ulnar shortening osteotomy may relieve the axial load on the TFCC.

Degenerative TFCC Tears— Degenerative Class II TFCC lesions are subclassified with subtypes based on the progressive destruction of the TFCC and adjacent ligaments and cartilage. Class IIA lesions represent wear of the horizontal portion of the disc proper without perforation. Class IIB lesions resemble IIA lesions with additional chondromalacia of the lunate and/or ulna. Progression of the degenerative change results in perforation of the disc proper, which then is classified as Class IIC lesions. Class IID lesions represent a further advanced degenerative process with rupture of the LTL **(Figure 10)**. Class IIE lesions describe the final stages of ulnar impaction syndrome. These findings are often associated with ulnocarpal and distal radioulnar degenerative arthritis. In the chronic phase of TFCC injury, conservative treatments are initially selected and, if unsuccessful, ulnar shortening osteotomy or ulnar head resection can be considered.[20]

A cadaveric study reported that TFCC degeneration begins in the third decade, and subsequent perforations increase with age.[21] Similarly, MRI findings of degenerative TFCC lesions were seen with higher frequency in patients older than 50.[22] Traumatic and degenerative abnormalities are difficult to distinguish between and can coexist as age increases.

Carpal Fractures

Carpal fractures account for 21% of upper extremity fractures, with the proximal carpal row most frequently affected.[23] While plain film radiographs remain the initial imaging modality of choice, early MRI has proven a valuable tool for radiographically occult fractures. MRI has sensitivity and specificity rates

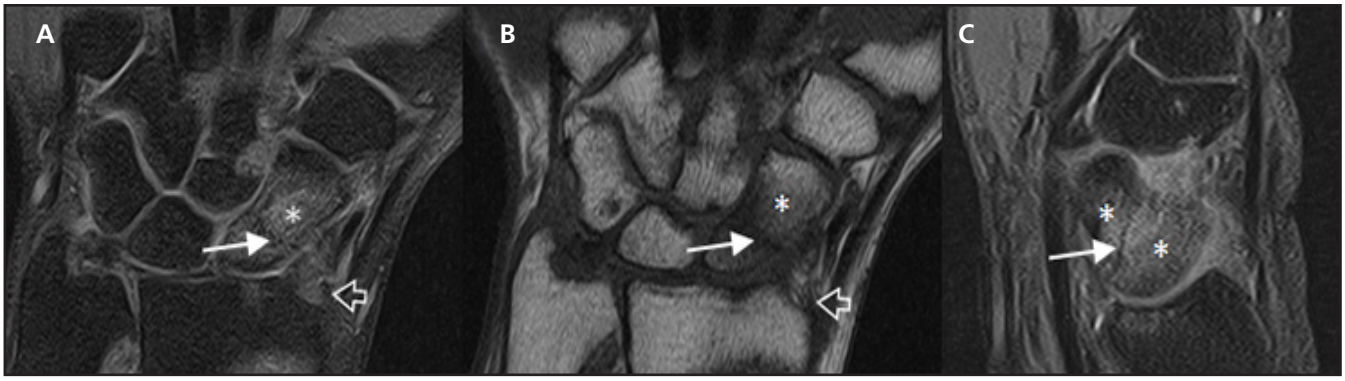

FIGURE 11. *Scaphoid fracture. Coronal FS PDWI (A) and Coronal T1WI (B) demonstrate a linear hypointense fracture line through the waist of the scaphoid (solid arrows) with adjacent reactive marrow edema (asterisks). Incidentally noted is a mildly displaced fracture of the radial styloid (open arrows). Sagittal FS PDWI (C) shows a linear hypointense fracture line through the scaphoid (solid arrow) with adjacent reactive edema (asterisks).*

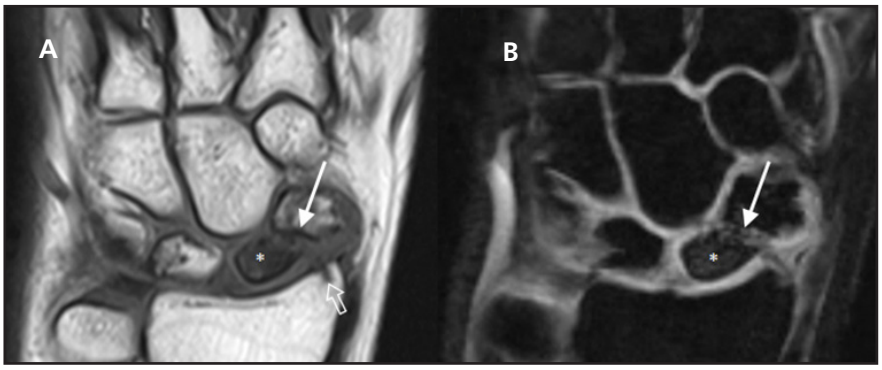

FIGURE 12. *Early scaphoid osteonecrosis. Coronal T1WI (A) shows a fracture through the waist of the scaphoid (solid arrow) with hypointense signal throughout the proximal pole (asterisk). Subtle degenerative change of the radiocarpal joint represent early scaphoid nonunion advanced collapse (SNAC wrist) (open arrow). Coronal 3D FS T2WI (B) shows a scaphoid waist fracture (solid arrow) with variable subtle increased signal throughout the proximal pole (asterisk).*

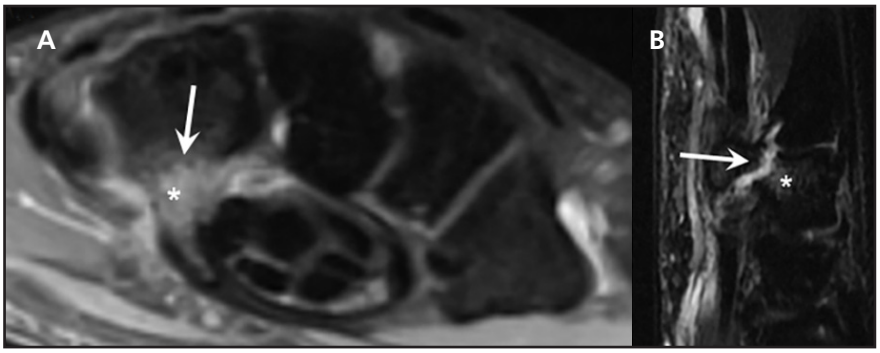

FIGURE 13. *Hamate fracture. Axial FS PDWI (A) shows fluid-like signal at the base of the hook of the hamate (solid arrow) with surrounding reactive edema (asterisk). Sagittal STIR image (B) shows linear hyperintense fracture through the base of the hook of the hamate (white arrow) with reactive edema with the body of the hamate (asterisk) and minimal displacement.*

of 80% and 100%, respectively, in radiographically occult scaphoid fractures.[24]

Carpal fractures exhibit a linear hypointensity on T1-weighted imaging (T1WI) with surrounding edema (T1-hypointensity and T2-hyperintensity). Short protocol MRI exams, consisting of short tau inversion recovery (STIR) and T1WI, have shown reliable negative predictive values in the acute setting often negating unnecessary immobilization and follow-up radiation.[25]

Scaphoid Fracture

The scaphoid is the most commonly fractured carpal bone, encompassing approximately 70% of all carpal fractures **(Figure 11)**. The scaphoid is divided into proximal, middle, and distal poles, which are important to delineate when predicting long-term healing potential. There is a single intraosseous artery (branch of the radial artery) to the scaphoid, which enters the scaphoid dorsally at the midpole (waist) and supplies the proximal pole in a retrograde fashion. While the majority of fractures heal with proper treatment, approximately 15% to 30% of scaphoid fractures will develop osteonecrosis, which increases in prevalence with proximal pole and displaced fractures.[26]

Up to 40% of scaphoid fractures are missed at initial presentation, and follow-up MRI of the wrist is becoming more common. A scaphoid fracture segment with hypointense T1- and T2-signal is concerning for decreased vascularity. While these findings alone are a poor predictor of impending osteonecrosis/nonunion, they should raise suspicion for potential setbacks in healing **(Figure 12)**.[27] As osteonecrosis develops, the scaphoid will exhibit fragmentation and collapse.

Treatment of scaphoid fractures is typically achieved conservatively with immobilization. Stable, nondisplaced fractures involving the mid/distal poles achieve a union rate of 90% with casting alone.[27] Surgery is commonly reserved for unstable or displaced fractures, proximal pole fractures, or when nonunion/osteonecrosis occurs.

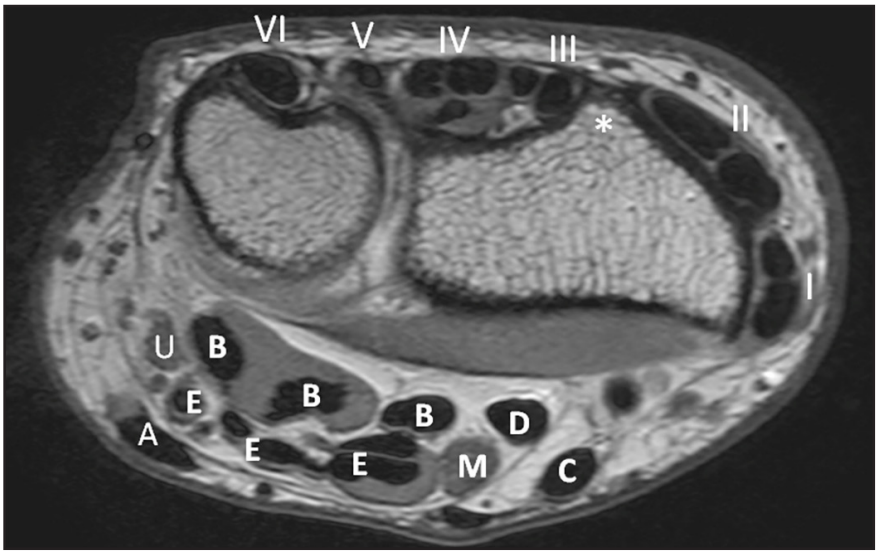

FIGURE 14. *The extensor tendon compartments and the flexor tendons. Axial PDWI displays Lister tubercle (asterisk), which serves as a landmark for the dorsal wrist. The extensor compartments are labeled with their respective Roman numerals I-VI. Extensor tendons within these compartments are: I = abductor pollicis longus and extensor pollicis brevis, II = extensor carpi radialis longus and brevis, III = extensor pollicis longus, IV = extensor digitorum and indicis, V = extensor digiti minimi, VI = extensor carpi ulnaris. The flexor tendons and the 2 nerves are also labelled and indicated in letters. A = flexor carpi ulnaris, B = flexor digitorum profundus, C = flexor carpi radialis, D = flexor pollicis longus, E = flexor digitorum superficialis, M = median nerve, U = ulnar nerve.*

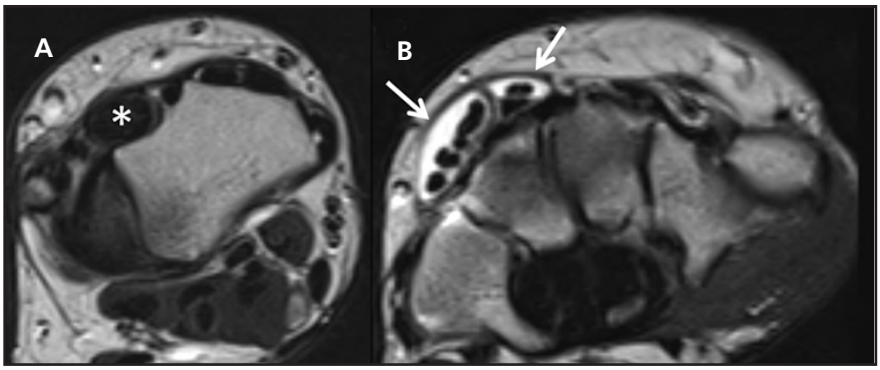

FIGURE 15. *Tendinopathy and tenosynovitis. Axial T2WI (A) shows focal thickening of the extensor compartment IV extensor digitorum and indicis tendons (asterisk), consistent with tendinopathy. Axial T2WI (B) shows fluid within the tendon sheaths of the extensor compartments III and IV (solid arrows), consistent with tenosynovitis.*

Triquetral Fracture

The triquetrum is the second-most commonly fractured carpal bone, accounting for 18.3% of carpal fractures.[28] They typically involve the dorsal cortex and are most frequently diagnosed on lateral radiographs of the wrist. Triquetral fractures are radiographically occult in up to 20% of cases.[28,29] On MRI, the most sensitive finding is bone marrow edema, which may even obscure the fracture line. Most commonly, the small fracture fragment is visualized within the dorsal soft tissues and follows the osseous signal on all sequences; however, diffuse soft-tissue edema may obscure these fragments.

It has been suggested that the dorsal fracture fragment results from a dorsal extrinsic ligament avulsion injury.[28] There is often combined ligamentous injury in these patients, which reinforces MRI's role in acute wrist injuries. Less frequent triquetral fractures involve the body of the triquetrum (typically in the setting of perilunate fracture dislocation) and volar avulsion fractures (ulnotriquetral or lunotriquetral ligament avulsion).

Hamate Fracture

Hamate fractures account for 1.7% of carpal fractures, with the hook of the hamate the most frequent site.[29] They are associated with racket sports as the handle directly compresses the protruding hook. Given the tendinous and ligamentous insertions on the hook of the hamate, associated displacement of the fragment may delay healing or nonunion. Occasionally, fractures may involve the body of the hamate, typically due to an axial loading injury or associated perilunate dislocations.[26]

MRI demonstrates a T1-hypointense and T2-hyperintense fracture line (**Figure 13**). Comment should be made on the degree of displacement and signal characteristics of the displaced fragment, as there is increased risk of nonunion when the hook of the hamate is involved.

Tendon Pathology

Normal Tendon Appearance

Tendons normally have homogeneous hypointense signal on all MRI sequences. Wrist tendons are divided into the flexor and extensor subgroups, and are best appreciated in the axial plane (**Figure 14**).[30] Most flexor tendons traverse the carpal tunnel, with 3 located outside the tunnel: the flexor carpi ulnaris, flexor carpi radialis, and the palmaris longus (PL) tendons. The PL is not present in a minority of the population. The extensor tendons are divided into 6 compartments, each with a separate tenosynovial sheath.[31]

General Tendon Abnormalities

Pathology of the wrist tendons include tendinopathy, tenosynovitis, and partial and complete tears. MRI allows the radiologist to reliably distinguish between these entities.

Tendinopathy is a generalized term describing diffuse or focal tendon thickening. This is usually secondary to chronic overuse and presents with T2-hyperintense signal within the tendon substance (**Figure 15A**).

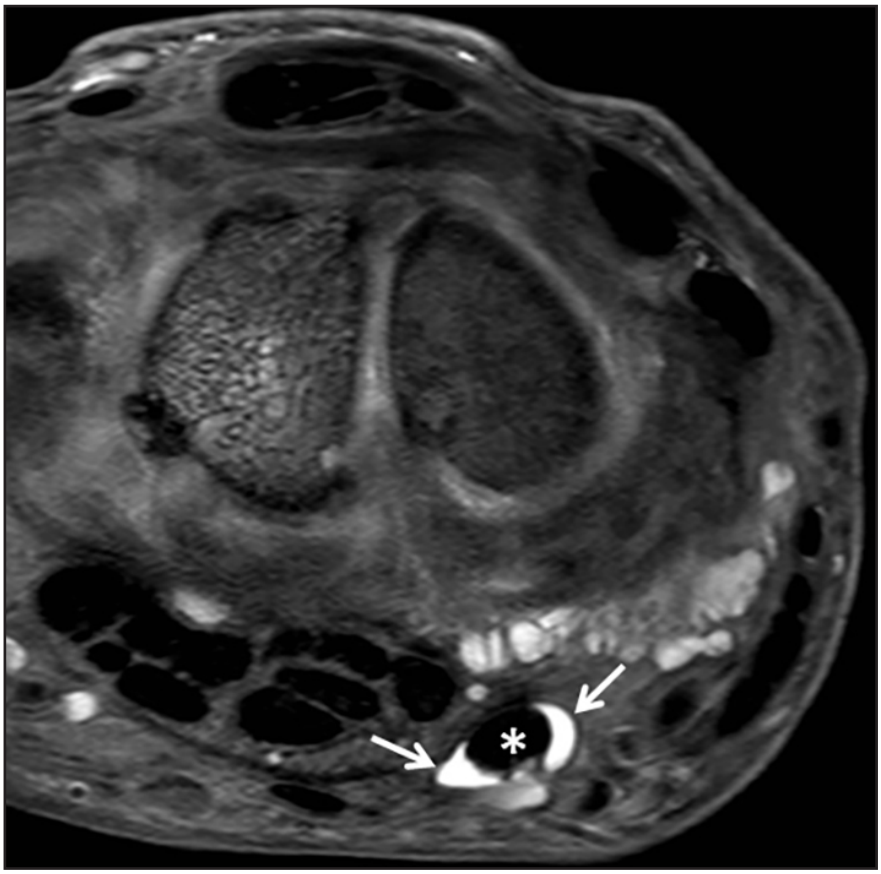

FIGURE 16. *Tenosynovitis of the flexor carpi radialis (FCR) tendon (asterisk). Axial FS PDWI displaying hyperintense fluid-like signal within the distended tendon sheath (arrows) of the FCR. The tendon sheath is distended and has an increased diameter compared to the tendon itself.*

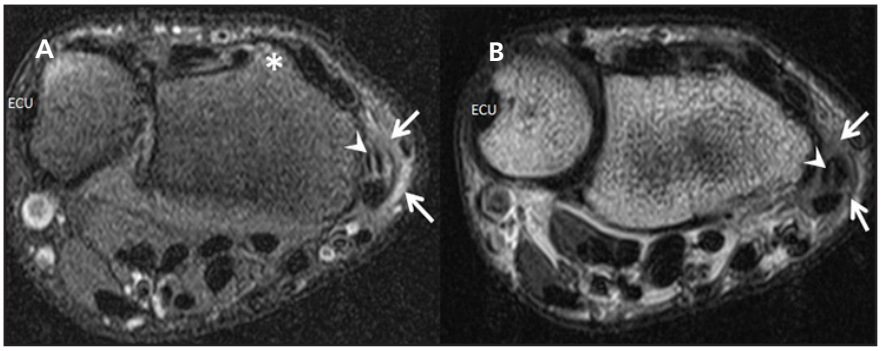

FIGURE 17. *Partial tendon tear. Axial FS PDWI (A) and axial PDWI (B) displaying interstitial hyperintense signal within the extensor pollicis brevis tendon (arrowhead). This is consistent with a partial interstitial split tear of the tendon. There is also peritendinous fluid-like signal and tendon sheath distention, consistent with de Quervain tenosynovitis (solid arrows). The anatomical landmark Lister tubercle is displayed (asterisk) as well as the extensor ECU.*

Tenosynovitis presents with a hyperintense fluid-signal within the tendon sheath **(Figures 15B, 16)**. The diameter of the tendon sheath fluid is greater than the tendon diameter. Fluid-like signal that does not surround the tendon is most commonly a normal finding. Usually patients with tenosynovitis or tendinopathy complain of localized tenderness, decreased grip strength, and pain with range of motion. These entities are usually related to repetitive trauma and inflammatory or infectious arthritis. Any wrist tendon may be affected; however, tendons at a point of restriction are most commonly involved (eg, the ECU tendon as it passes over the ulnar groove). They are often successfully treated with conservative therapy.

MRI findings of a torn tendon include a focal disruption or distorted appearance of the tendon. *Partial tears* have a focal region of hyperintense T1- and T2-signal with some fibers remaining intact **(Figure 17)**. *Complete tears* show full-thickness discontinuity at any point of the tendon and often present with retraction of the torn tendon. Peritendinous edema and/or hemorrhage suggest an acute tear. Tendon tears are often treated conservatively with splinting. However, if conservative treatment fails or the tear is > 40% thickness of the tendon, primary surgical repair is often performed.[30]

de Quervain Tenosynovitis

First described in 1895, this condition is a stenosing tenosynovitis affecting the extensor pollicis brevis (EPB) and abductor pollicis longus (APL) tendons of the wrist.[30,32,33] This results from chronic overuse and can commonly be seen in women (particularly new mothers), racquet sports, golf, and also recently recognized in frequent texters.

Patients present with pain along the radial aspect of the wrist exacerbated by thumb adduction and ulnar deviation of the wrist. There can be localized swelling and tenderness. The Finkelstein test is positive when pain occurs upon passive ulnar deviation while the thumb is adducted.

MRI displays EPB and APL tenosynovitis with fluid-like signal within the tendon sheath. Associated tendinopathy varies from localized tendon thickening to an interstitial tear. Peritendinous edema-like signal also often surrounds the first extensor compartment **(Figure 18)**.

Treatment begins conservatively with nonsteroidal anti-inflammatory drugs (NSAIDS) and immobilization with a thumb spica brace. Corticosteroid injection into the first dorsal compartment can also yield good results. Surgical decompression is reserved for patients who fail these measures.

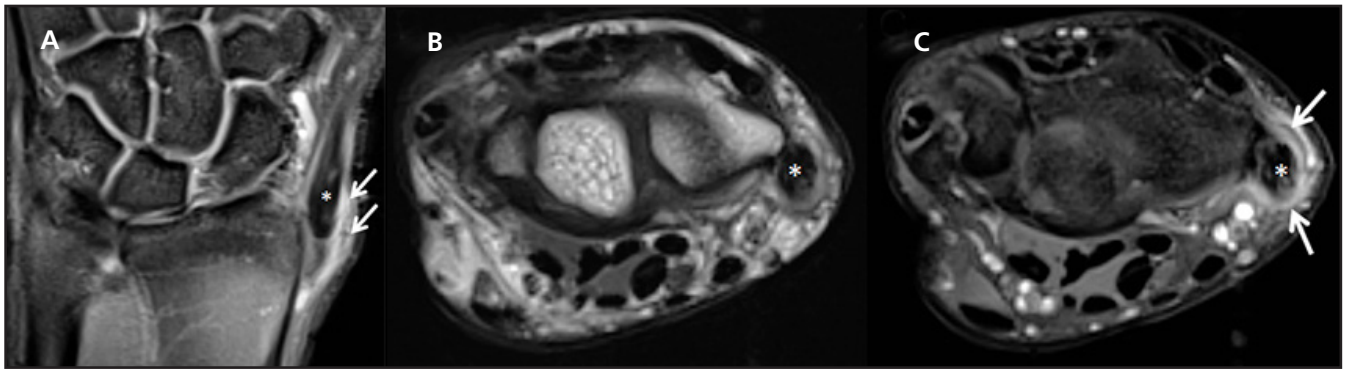

FIGURE 18. *de Quervain tenosynovitis. Coronal FS PDWI (A), axial PDWI (B), and axial FS PDWI (C) of the wrist. Fluid-like signal within the thickened extensor pollicis brevis and abductor pollicis longus tendons consistent with tendinopathy (asterisk). There is fluid within the tendon sheaths (tenosynovitis) and adjacent soft tissues (arrows).*

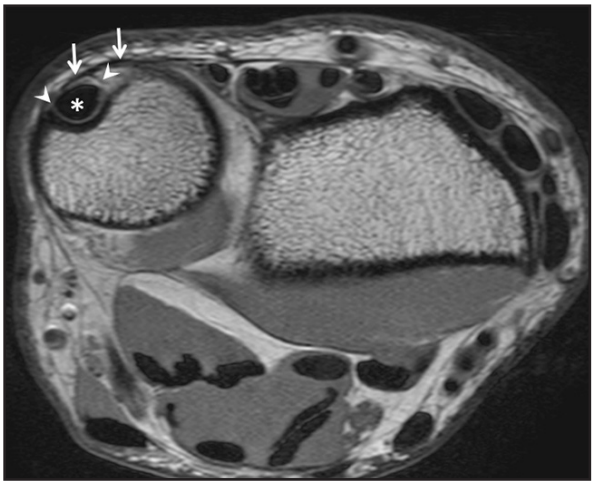

FIGURE 19. *ECU tendon. Single axial PDWI at the level of the distal ulna showing the ECU subsheath (arrowheads) deep to the overlying extensor retinaculum (solid arrows). The ECU subsheath and extensor retinaculum form the fibro-osseous tunnel for the ECU and blend together along the dorsal aspect. The normal ECU tendon is seen (asterisk) and has normal diffusely low-signal intensity.*

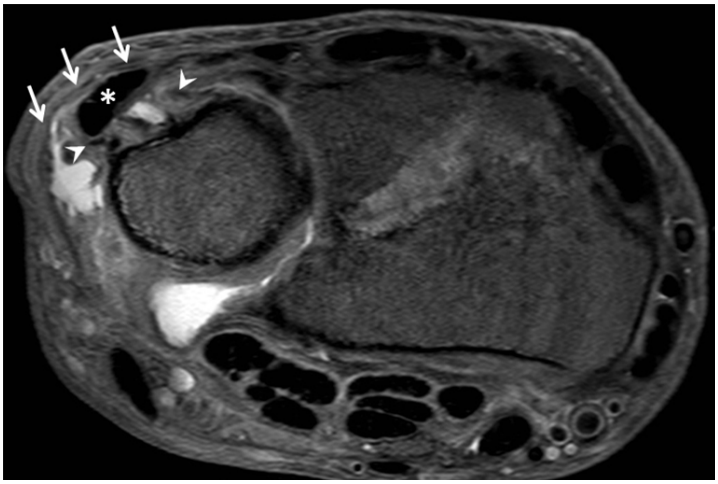

FIGURE 20*. ECU subsheath tear at both the dorsal and volar attachments with subluxation of the ECU tendon. Single axial FS PDWI demonstrating a subluxed ECU tendon (asterisk), which lies dorsal and ulnar to the disrupted subsheath (arrowheads). The subsheath is diffusely thickened and laxed in appearance with tenosynovitis present. The extensor retinaculum remains intact (solid arrows).*

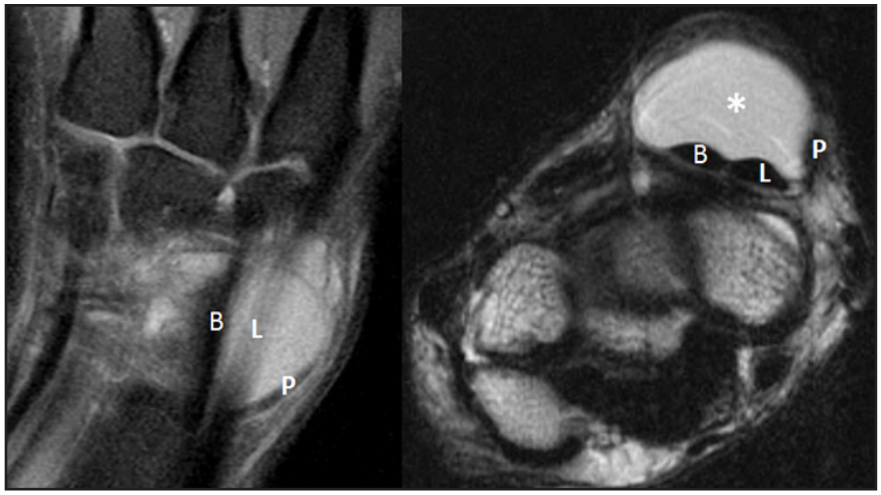

FIGURE 21. *Coronal FS PDWI (A) and axial T2WI (B) in the distal intersection syndrome of the wrist. The displaced extensor pollicis longus tendon (P) crossing over the extensor carpi radialis longus (L) and extensor carpi radialis brevis (B) tendons. The tendon sheath of L and B is markedly distended with fluid-like signal (asterisk), as there is friction between the crossing tendons.*

Extensor Carpi Ulnaris Injuries

The ECU has unique anatomical characteristics and courses along the dorsomedial aspect of the forearm through its own fibro-osseous tunnel, in a groove between the ulnar head and the styloid process.[10,14,34] This tunnel is formed by the distal ulna and a band of connective tissue known as the ECU subsheath, which stabilizes the ECU as it courses over the distal ulna **(Figure 19)**. The combination of the subsheath and extensor retinaculum prevent subluxation and friction of the ECU tendon.

Extensor Carpi Ulnaris Tenosynovitis and Tendinosis

These entities occur from repetitive stress causing synovial inflammation

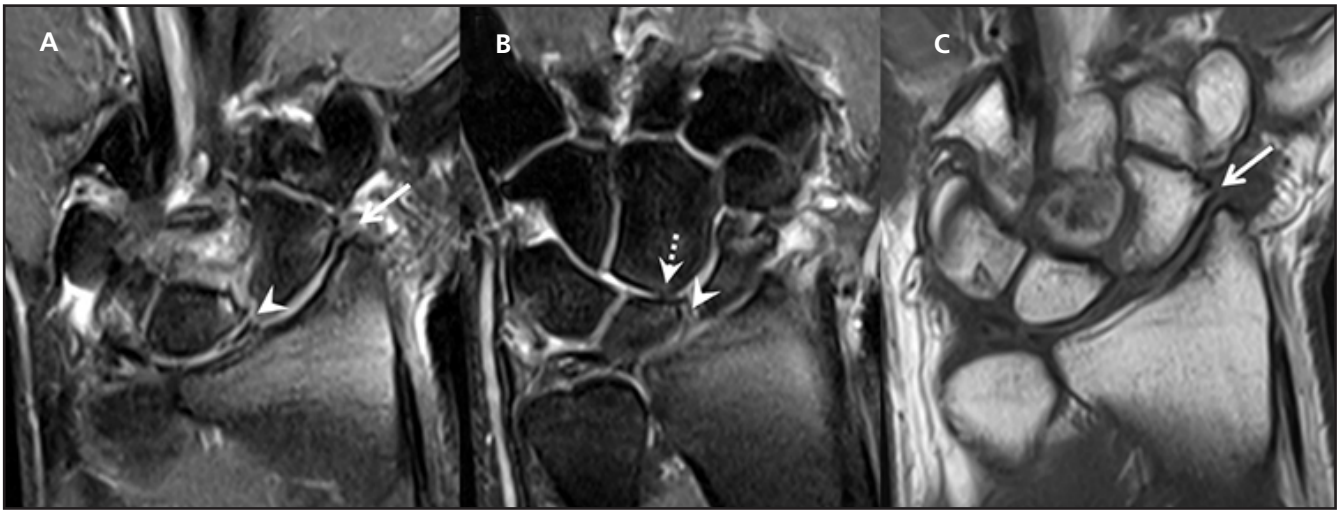

FIGURE 22. *SLAC wrist. Coronal FS PDWI (A and B) and a single coronal T1WI (C). There is a partial proximal segment tear of the SLL (arrowheads, A and B) with joint space narrowing, sclerosis, and osteophyte formation of the radioscaphoid joint. This is most significant along the radial styloid (solid arrows, A and C). There is joint space loss (dashed arrow, B) and sclerosis of the capitolunate joint, suggesting stage III disease.*

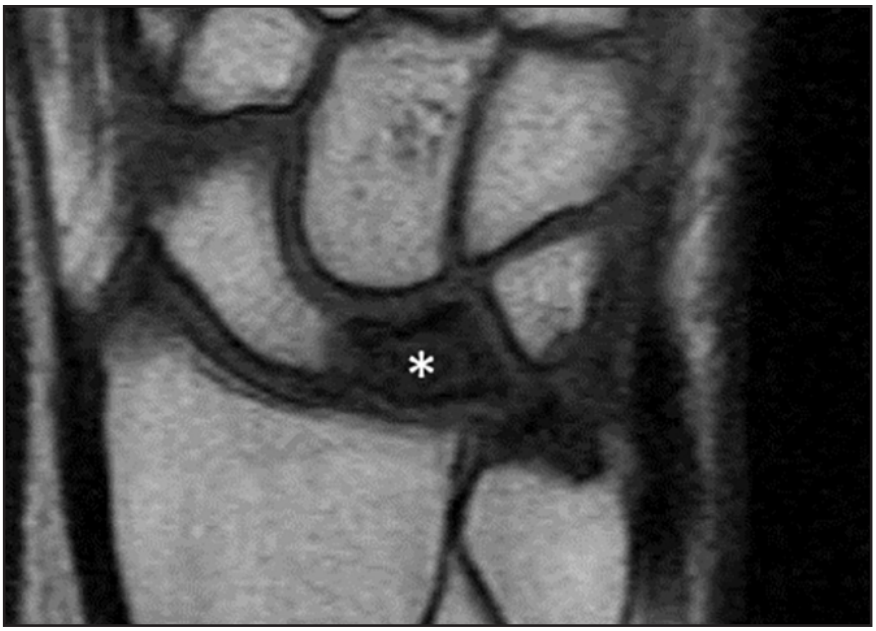

FIGURE 23. *Kienbock's disease. Coronal T1WI displays homogeneous T1-hypointensity throughout the lunate without collapse (asterisk). This is consistent with Lichtman stage II classification. This process follows a progression with stage III disease having early collapse of the lunate, and stage IV displaying continued collapse with radiocarpal and midcarpal degenerative joint disease.*

and are commonly seen in athletes, particularly rowers and racquet sport players. Typical presentation includes point tenderness and swelling at the dorsal/ulnar aspect of the wrist.

Progression usually begins with tenosynovitis and circumferential hyperintense T2-signal on MRI. Continued stress leads to tendinopathy and ultimately tendon tear.[9] A pitfall on MRI is the "pseudolesion," which is when the tendon has centrally increased T1- and T2-signal on axial images at the level of the distal radioulnar joint (DRUJ). This is secondary to intrasubstance mucoid degeneration or magic angle effect.[1,35] Nonfocal increased signal and tendon thickening distinguish true tendinosis from a pseudolesion.

Nonsurgical conservative treatment is often successful with splinting of the wrist for 6 to 8 weeks. If this fails, surgical release of the sixth compartment can be performed with tendon debridement and subsheath reconstruction.

Extensor Carpi Ulnaris Subsheath Injury

The ulnar wall of the subsheath can rupture in the setting of trauma or with recurrent stress injuries. This often results in ECU subluxation, with ulnar displacement of the tendon, even if the overlying extensor retinaculum is intact.[9,30] The tendon commonly returns to a normal position in pronation. On MRI, the ECU is subluxed with complete tears of the ECU subsheath dorsal attachment. The volar attachment of the ECU subsheath is often lax and there is usually peritendinous edema **(Figure 20)**.

Intersection Syndrome

There are 2 intersection syndromes involving the extensor tendons second compartment.[31,36] The *distal intersection syndrome* involves the extensor pollicis longus (EPL) as it crosses over the extensor carpi radialis longus (ECRL) and extensor carpi radialis brevis (ECRB) tendons, and is rare **(Figure 21)**. The more common *proximal intersection syndrome* involves the APL and EPB myotendinous junctions as they cross over the ECRL and ECRB. This occurs approximately 4 to 8 cm

proximal to the Lister tubercle and is known as the "oarsmen's wrist," commonly affecting rowers and weightlifters as a result of repetitive wrist flexion/extension. MRI shows tenosynovitis involving the tendon with surrounding soft-tissue, edema-like signal.[36]

These intersection syndromes are commonly treated conservatively with steroid or local anesthetic injection into the second compartment. If this fails, tenosynovectomy and decompression can be performed at the level of intersection.

Scapholunate Advanced Collapse (SLAC) and Scaphoid Nonunion Advanced Collapse (SNAC)

These entities represent the most common types of wrist arthritis seen by hand surgeons.[37] Given their prevalence and associated disability, it is important to recognize them radiographically. MRI is unnecessary for staging the disease, but displays cartilage to a much better extent.[38]

SLAC wrist pattern of osteoarthritis occurs after injury or degenerative attenuation of the SLL. SNAC wrist develops following a scaphoid fracture that progresses to nonunion. There is a traditional 4-stage classification scheme of SLAC and SNAC wrists.[39] Stage I displays arthrosis at the radial styloid-distal scaphoid articulation. Stage II involves the proximal radioscaphoid joint in SLAC wrists and the scaphocapitate joint in SNAC wrists. Stage III involves degeneration of the midcarpal joint, and specifically the capitolunate joint **(Figure 22)**. Stage IV involves pancarpal arthrosis with preservation of the radiolunate joint.

Kienbock disease

Kienbock disease is avascular necrosis of the lunate (lunatomalacia or lunate osteonecrosis). The most common theory for this entity is compromise of the lunate vasculature.[40] Risk factors associated with Kienbock disease include negative ulnar variance, high uncovering of the lunate, abnormal radial inclination, and trapezoidal shape of the lunate.[41] Without prompt diagnosis and treatment, disease progression will ultimately lead to joint destruction within 3 to 5 years.[40]

The pattern of disease follows a progression delineated by the Lichtman classification, staging by lunate morphology and signal characteristics **(Figure 23)**. In *stage I*, the lunate maintains its normal morphology, but develops a uniform edema-like pattern of diffuse T1-weighted hypointensity and hyperintense signal on fluid-sensitive sequences. *Stage II* denotes the early sclerotic changes of the lunate with hypointense signal on T1WI and variable signal on fluid-sensitive sequences. Stage II also marks the earliest findings on plain film radiography with increased density of the lunate. Progression to collapse is first demonstrated in *stage III* with loss of height in the coronal plane and lengthening of the lunate in the sagittal plane. *Stage IV* is characterized by lunate collapse along with radiocarpal and midcarpal degenerative change. In addition, an adjacent reactive synovitis and joint effusion may be associated.[40] If intravenous gadolinium is used during imaging, nonenhancing portions of the lunate are concerning for nonviable fragments, although late revascularization may occur.

Conclusion

MRI of the wrist is progressively increasing in utilization, but is often a daunting task for interpreting radiologists. Understanding the complex anatomy of the wrist and more common disease of the ligamentous, osseous, and tendinous structures allows the radiologist to efficiently and accurately evaluate MRI of the wrist with improved diagnostic capabilities. This ultimately leads to more efficient treatment and better patient outcomes.

References

1.Burns JE, Tanaka T, Ueno T, et al. Pitfalls that may mimic injuries of the triangular fibrocartilage and proximal intrinsic wrist ligaments at MR imaging. Radiographics 2011;31(1):63-78.

2.Ringler MD, Murthy NS. MR Imaging of wrist ligaments. Magn Reson Imaging Clin N Am 2015;23(3):367-391.

3.Tanaka T, Ogino S, Yoshioka H. Ligamentous injuries of the wrist. Semin Musculoskelet Radiol 2008;12(4):359-377.

4.Bateni CP, Bartolotta RJ, Richardson ML, et al. Imaging key wrist ligaments: what the surgeon needs the radiologist to know. Am J Roentgenol 2013;200(5):1089-1095.

5.Hafezi-Nejad N, Carrino JA, Eng J, et al. Scapholunate interosseous ligament tears: diagnostic performance of 1.5 T, 3 T MRI, and MR arthrography—a systematic review and meta-analysis. Acad Radiol 2016;23(9):1091-1103.

6.Elsaftawy A, Jabłecki J, Jurek T, et al. New concept of scapholunate dissociation treatment and novel modification of Brunelli procedure—anatomical study. BMC Musculoskelet Disord 2014;15:172.

7.Magee T. Comparison of 3-T MRI and arthroscopy of intrinsic wrist ligament and TFCC tears. Am J Roentgenol 2009;192(1):80-85.

8.Asaad AM, Andronic A, Newby MP, et al. Diagnostic accuracy of single-compartment magnetic resonance arthrography in detecting common causes of chronic wrist pain. J Hand Surg Eur Vol 2017;42(6):580-585.

9.Watanabe A, Souza F, Vezeridis PS, et al. Ulnar-sided wrist pain. II. Clinical imaging and treatment. Skeletal Radiol 2010;39(9):837-857.

10. Vezeridis PS, Yoshioka H, Han R, et al. Ulnar-sided wrist pain. Part I: anatomy and physical examination. Skeletal Radiol 2010;39(8):733-745.

11. Taneja AK, Bredella MA, Chang CY, et al. Extrinsic wrist ligaments: prevalence of injury by magnetic resonance imaging and association with intrinsic ligament tears. J Comput Assist Tomogr 2013;37(5):783-789.

12. Kirchberger MC, Unglaub F, Mühldorfer-Fodor M, et al. Update TFCC: histology and pathology, classification, examination and diagnostics. Arch Orthop Trauma Surg 2015;135(3):427-437.

13. Cody ME, Nakamura DT, Small KM, et al. MR Imaging of the triangular fibrocartilage complex. Magn Reson Imaging Clin N Am 2015;23(3): 393-403.

14. von Borstel D, Wang M, Small K, et al. High-resolution 3T MR Imaging of the triangular fibrocartilage complex. Magn Reson Med Sci 2017;16(1): 3-15.

15. Yoshioka H, Burns JE. Magnetic resonance imaging of triangular fibrocartilage. J Magn Reson Imaging 2012;35(4):764-778.

16. Wang ZX, Chen SL, Wang QQ, et al. The performance of magnetic resonance imaging in the detection of triangular fibrocartilage complex injury: a meta-analysis. J Hand Surg Eur Vol 2015;40(5): 477-484.

17. Smith TO, Drew B, Toms AP, et al. Diagnostic accuracy of magnetic resonance imaging and magnetic resonance arthrography for triangular fibrocartilaginous complex injury: a systematic review and meta-analysis. J Bone Joint Surg Am 2012;94(9):824.

18. Chang AL, Yu HJ, von Borstel D, et al. Advanced imaging techniques of the wrist. Am J Roentgenol 2017;209(3):497-510.

19. Palmer AK. Triangular fibrocartilage complex lesions: a classification. J Hand Surg Am 1989;14(4):594-606.

20. Minami A. Triangular fibrocartilage complex tears. Hand Surg 2015;20(1):1-9.

21. MikićZD. Age changes in the triangular fibrocartilage of the wrist joint. J Anat 1978;126(Pt 2): 367-384.

22. Nozaki T, Rafijah G, Yang L, et al. High-resolution 3 T MRI of traumatic and degenerative triangular fibrocartilage complex (TFCC) abnormalities using Palmer and Outerbridge classifications. Clin Radiol 2017;72(10):904.e1-e904.e10.
23. Ootes D, Lambers KT, Ring DC. The epidemiology of upper extremity injuries presenting to the emergency department in the United States. Hand 2012;7(1):18-22.
24. Beeres FJP, Rhemrev SJ, den Hollander P, et al. Early magnetic resonance imaging compared with bone scintigraphy in suspected scaphoid fractures. J Bone Joint Surg Br 2008;90(9):1205-1209.
25. Kanavaki A, Draenert C, Ceroni D, et al. Short MRI protocol for excluding traumatic lesions of the scaphoid bone in children. In Vivo 2016;30(4): 495-499.
26. Kaewlai R, Avery LL, Asrani AV, et al. Multidetector CT of carpal injuries: anatomy, fractures, and fracture-dislocations. Radiographics 2008;28(6):1771-1784.
27. Dawson JS, Martel AL, Davis TR. Scaphoid blood flow and acute fracture healing. A dynamic MRI study with enhancement with gadolinium. J Bone Joint Surg Br 2001;83(6):809-814.
28. Becce F, Theumann N, Bollmann C, et al. Dorsal fractures of the triquetrum: MRI findings with an emphasis on dorsal carpal ligament injuries. Am J Roentgenol 2013;200(3): 608-617.
29. Welling RD, Jacobson JA, Jamadar DA, et al. MDCT and radiography of wrist fractures: radiographic sensitivity and fracture patterns. Am J Roentgenol 2008;190(1):10-16.
30. Plotkin B, Sampath SC, Sampath SC, et al. MR imaging and US of the wrist tendons. Radiographics 2016;36(6):1688-1700.
31. Meraj S, Gyftopoulos S, Nellans K, et al. MRI of the extensor tendons of the wrist. Am J Roentgenol 2017;209(5):1093-1102.
32. Lok RLK, Griffith JF, Ng AWH, et al. Imaging of radial wrist pain. Part II: pathology. Skeletal Radiol 2014;43(6):725-743.
33. Cockenpot E, Lefebvre G, Demondion X, et al. Imaging of sports-related hand and wrist injuries: sports imaging series. Radiology 2016;279(3): 674-692.
34. Henderson CJ, Kobayashi KM. Ulnar-sided wrist pain in the athlete. Orthop Clin North Am 2016;47(4):789-798.
35. Ali S, Cunningham R, Amin M, et al. The extensor carpi ulnaris pseudolesion: evaluation with microCT, histology, and MRI. Skeletal Radiol 2015;44(12):1735-1743.
36. de Lima JE, Kim H-J, Albertotti F, et al. Intersection syndrome: MR imaging with anatomic comparison of the distal forearm. Skeletal Radiol 2004;33(11):627-631.
37. Watson HK, Ballet FL. The SLAC wrist: scapholunate advanced collapse pattern of degenerative arthritis. J Hand Surg Am 1984;9(3): 358-365.
38. Li AE, Lee SK, Rancy SK, et al. Comparison of Magnetic Resonance Imaging and Radiographs for Evaluation of Carpal Osteoarthritis. J Wrist Surg 2017;6(2):120-125.
39. Shah CM, Stern PJ. Scapholunate advanced collapse (SLAC) and scaphoid nonunion advanced collapse (SNAC) wrist arthritis. Curr Rev Musculoskelet Med 2013;6(1):9-17.
40. Arnaiz J, Piedra T, Cerezal L, et al. Imaging of Kienböck disease. Am J Roentgenol 2014;203(1):131-139.
41. Lutsky K, Beredjiklian PK. Kienböck Disease. J Hand Surg Am 2012;37(9):1942-1952.